Structural and transport measurements in $La_{1.8}Sr_{0.2}NiO_{4+\delta}$

S. A. Hoffman
Department of Physics, Purdue University, West Lafayette, Indiana 47907

C. Venkatraman and S. N. Ehrlich
Department of Materials Science and Engineering, Purdue University, West Lafayette, Indiana 47907

S. M. Durbin
Department of Physics, Purdue University, West Lafayette, Indiana 47907

G. L. Liedl
Department of Materials Science and Engineering, Purdue University, West Lafayette, Indiana 47907
(Received 10 September 1990)

Lattice constants, electrical resistivity, and magnetization have been measured as a function of temperature on single crystals of $La_{1.8}Sr_{0.2}NiO_{4+\delta}$, a nickelate analog of lanthanum strontium cuprate, the 40-K superconductor. Diamagnetism was observed at 4.2 K, but not zero resistance. The oxygen concentration was carefully controlled to probe the region close to stoichiometric lanthanum strontium nickelate, from $\delta=0.001$ to 0.003. The high-temperature tetragonal structure persists down to near 100 K, with semiconductorlike resistivity showing activation energies between 32 and 54 meV, depending on δ. Below 100 K the structure transforms into a low-temperature orthorhombic phase, often displaying distinct, cycling-dependent changes in activation energies. In some specimens the resistance occasionally fell by several orders of magnitude, but recovered to previous values within a few degrees. X-ray-diffraction rocking curves reveal striking changes in the mosaic spread of these specimens as a function of both time and temperature, which helps explain the irreproducibility of the activation energies and the resistance anomalies. Although no further structural changes are observed, the paramagnetic susceptibility goes through a maximum at 20 K. Consistent with previous reports, the magnetic remanence becomes finite below 20 K and the susceptibility decreases, sometimes becoming diamagnetic above 4.2 K. The activation energy in this phase abruptly decreases to only 5 meV, while the resistivity exceeds 10^{10} Ω cm. No evidence of zero resistance was found.

I. INTRODUCTION

The discovery of high-temperature superconductivity in lanthanum strontium cuprate[1] has led to renewed interest in the isostructural nickel-based oxides, lanthanum strontium nickelate ($La_{2-x}Sr_xNiO_{4+\delta}$).[2-4] These nickelates themselves became candidates for possible superconductivity with the surprising discovery of diamagnetism in $La_{1.80}Sr_{0.2}NiO_{4+\delta}$ and undoped $La_2NiO_{4+\delta}$ by Kakol, Spałek, and Honig.[5,6] We report here on a series of measurements of resistivity, magnetization, and x-ray structure on single-crystal specimens of $La_{1.8}Sr_{0.2}NiO_{4+\delta}$ very near stoichiometric oxygen concentrations, i.e., for $0.001 \leq \delta \leq 0.003$. With regard to possible superconductivity, we have found diamagnetism but without zero resistance. A transition from tetragonal to orthorhombic structure near 100 K with subsequent change in mosaic structure may explain some of the difficulty in achieving reproducible results.

II. CRYSTAL PREPARATION

The single-crystal specimens of $La_{1.80}Sr_{0.20}NiO_{4+\delta}$ used in this study were obtained from a large boule grown by the crucible-free skull melter technique.[7] This same boule was the source of specimens exhibiting diamagnetism as reported in Ref. 5. Specimens were oriented using a Laue x-ray camera, and cut into rectangular plates approximately $4\times2\times1\,mm^3$ with a diamond saw. The amount of excess oxygen δ was fixed by anneals at 1000 °C in a controlled atmosphere of CO-CO_2. The oxygen partial pressure was monitored with a calibrated oxygen fugacity cell, with typical values of $P_{O_2}=10^{-11.5}$ atm. The relationship between δ and P_{O_2} at a given temperature was determined by thermogravimetric analysis.[8] The estimated uncertainty in δ is 0.001. After quenching, the specimen surfaces were ground to remove any surface layers which may have formed with a different oxygen concentration during the quench. Crystals were stored under dry mineral oil to inhibit permeation by oxygen and water, and measurements were made promptly whenever possible.

III. STRUCTURE

A significant amount of structural characterization has now been done for both the lanthanum nickelates and the cuprates, with various strontium-, barium-, and oxygen-

doping levels.[4,9–15] Because of their similarities, and because various authors use different conventions for describing these structures, we shall begin with an overview of this subject.

The "parent" structure for all of these compounds is the K_2NiF_4 structure, which has a body-centered tetragonal Bravais lattice and the $I4/mmm$ space group (or D_{4h}^{17}, No. 139 in the International Tables).[16] The unit cell of tetragonal La_2NiO_4 is shown in Fig. 1(a). All of the lanthanum nickelates and cuprates considered here have this structure at high temperatures, which we denote by HTT for "high-temperature tetragonal." These compounds transform to a low-temperature orthorhombic (LTO) phase through a distortion in the tetragonal [110] direction. To illustrate this point, we first show in Fig. 1(b) an extension of the body-centered tetragonal Bravais lattice as a face-centered tetragonal lattice. The **a** and **b** lattice vectors point along the tetragonal [110] and [$\bar{1}$10] directions, respectively. The orthorhombic phase simply corresponds to a change in length of **a** with respect to **b**, with their directions unchanged.

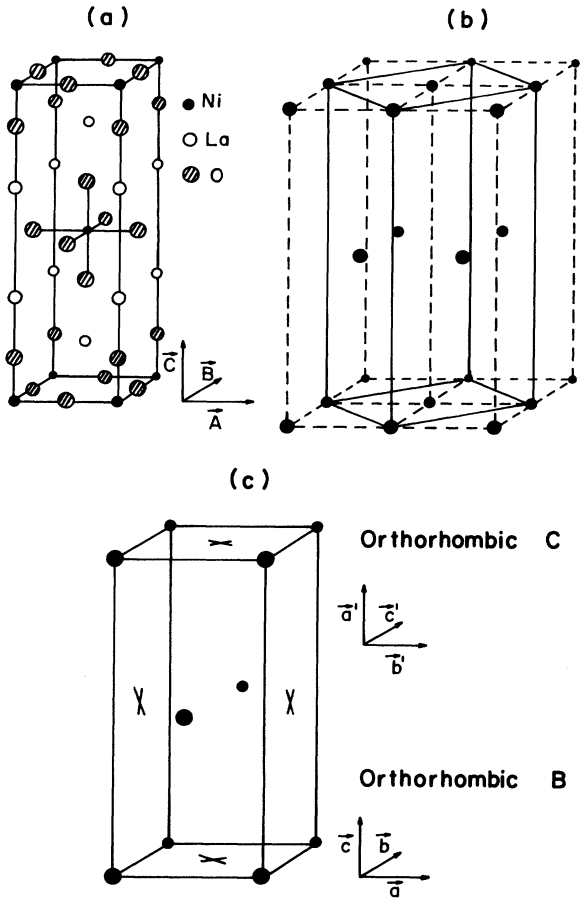

FIG. 1. Structure and Bravais lattices for lanthanum strontium nickelate. (a) Arrangement of Ni, La, and O atoms in the K_2NiF_4 body-centered tetragonal structure ($A=B\neq C$). Strontium doping occurs at the La sites. (b) Four adjacent unit cells of the K_2NiF_4 body-centered tetragonal Bravais lattice are shown by dashed lines, with the positions of the Ni atoms indicated. The solid-line unit cell shows the face-centered tetragonal lattice which can describe the same structure. (c) The orthorhombic Bravais lattice derived from the face-centered tetragonal unit cell shown above. The face-centered Ni atoms are no longer all equivalent due to a rearrangement of neighboring oxygen atoms; these inequivalent sites are denoted by crosses. This one-face-centered Bravais lattice can be described as either orthorhombic *C* or orthorhombic *B*, as illustrated by the corresponding unit vector directions.

This simple distortion changes the face-centered tetragonal lattice into a face-centered orthorhombic Bravais lattice [Fig. 1(c)]. The LTO phase is somewhat more complicated, however, in that only one of the unit-cell faces is actually centered. If the orthorhombic structure is derived from the tetragonal as above, it is natural to choose the centered face to be in the **a**-**c** plane (or, equivalently, the **b**-**c** plane), and the Bravais lattice is orthorhombic *B*. The usual convention in crystallography, however, is to choose the settings of the **a**, **b**, and **c** axes so that the centered face lies in the **a**-**b** plane, which then becomes an orthorhombic-*C* Bravais lattice.[17] It is just this choice of settings which distinguishes the *Bmab* and *Cmca* space groups which are both used to describe the same LTO structure.

For pure La_2NiO_4, the HTT-LTO transition occurs near 700 K.[18] The corresponding transition temperature for a specimen with $\delta=0.05$ is $T=240$ K,[2,3,19] which illustrates the importance of precise control of the oxygen concentration. Several groups have determined the space group of the LTO phase to be *Bmab* (or, equivalently, *Cmca*).[4,10,11,18] Neutron studies on powder samples[4,11] and single crystals[10] find a new phase below 80 K, in which the LTO structure reverts to being tetragonal again, i.e., there is a reentrant low-temperature tetragonal phase (LTT).

Nearly identical behavior has been seen in the lanthanum cuprates. For pure La_2CuO_4, the HTT-LTO transition occurs near 533 K.[20,21] In the barium-doped compounds $La_{2-x}Ba_xCuO_4$, this transition temperature falls linearly to less than 50 K as x increases to 0.20. The reentrant LTO-LTT transformation occurs below 80 K for $0.05\leq x\leq 0.125$.[15]

No previous structural studies of Sr-doped lanthanum nickelates have been reported. One purpose of our work was to determine if the reported diamagnetism[5,6] was correlated with a structural phase transformation. We performed x-ray-diffraction measurements at the National Synchrotron Light Source (NSLS) at Brookhaven National Laboratory, using the Matrix beamline, X-18a. An oriented single crystal of $La_{1.8}Sr_{0.20}NiO_{4.002}$ was mounted to the cold finger of a closed-cycle refrigerator, and wires were attached to the crystal to permit four-point resistance measurements. Diffraction measurements were made between room temperature and 8.5 K, using a standard six-circle diffractometer equipped with a Ge(111) analyzing crystal. Using the orthorhombic-*B* setting to define the Miller indices, we were able to measure a (200) reflection and its (020) twinned counterpart, the (220) reflection, and the (404) reflection. This very limited data set cannot be used to determine space groups, of course, but it is quite sensitive to the HTT-LTO transition.

Only one peak is seen at the (200) reflection at room temperature, consistent with the tetragonal structure. Below 100 K, however, a splitting becomes readily apparent. We interpret the two peaks as being the (200) and (020) orthorhombic Bragg peaks due to the two possible orientations of domains. These two peaks are slightly rotated about the c axis, consistent with a (110) twinning plane. We fit these peaks with a standard line shape,[22] and calculate the a-b lattice constants as a function of temperature. As shown in Fig. 2, the extrapolation of these data indicate a HTT-LTO transition at 100±3 K. Although measured for only one value of x, the large change in transition temperature with Sr content is similar to the behavior observed in Ba-doped lanthanum cuprate.[15] Note that there is no evidence for a reentrant LTO-LTT transition down to 8.5 K.

Because the tetragonal structure can become orthorhombic by distorting in either of two equivalent directions, in this case the tetragonal [110] and [$\bar{1}$10] (or orthorhombic [100] and [010] directions), domains of two possible orientations can form. The misfit between these domains can alter the mosaic structure of the specimen in a manner dependent upon both temperature and thermal cycling history. In Fig. 3 we show the results of various rocking curve scans obtained by rotating the crystal about the [$\bar{1}$10] (orthorhombic-B) axis while measuring the (220) diffracted intensity. Note that the room-temperature scans before and after one cycle to low temperature are similar, but not identical. Below the HTT-LTO transition, this mosaic structure changes drastically with temperature cycling, as seen in the two 90-K plots in Fig. 3. These variations suggest that the amount of mo-

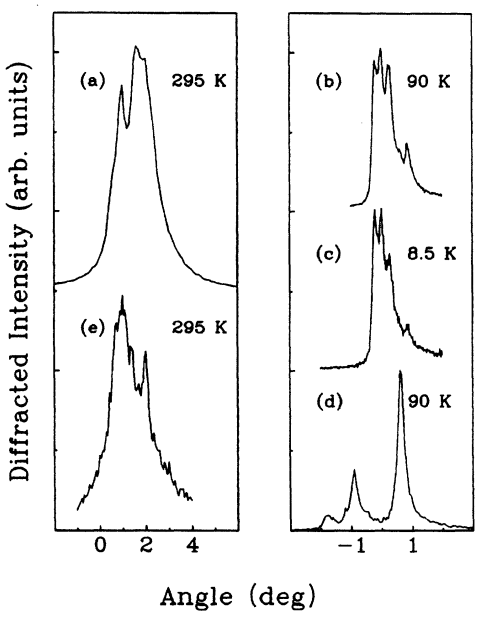

FIG. 3. Rocking curve scans of the (220) reflection (orthorhombic B) obtained by rotating about the [$\bar{1}$10] axis. All curves are taken from the same specimen as it was cycled through the following temperatures: (a) room temperature, (b) 90 K, (c) 8.5 K, (d) 90 K, and (e) room temperature.

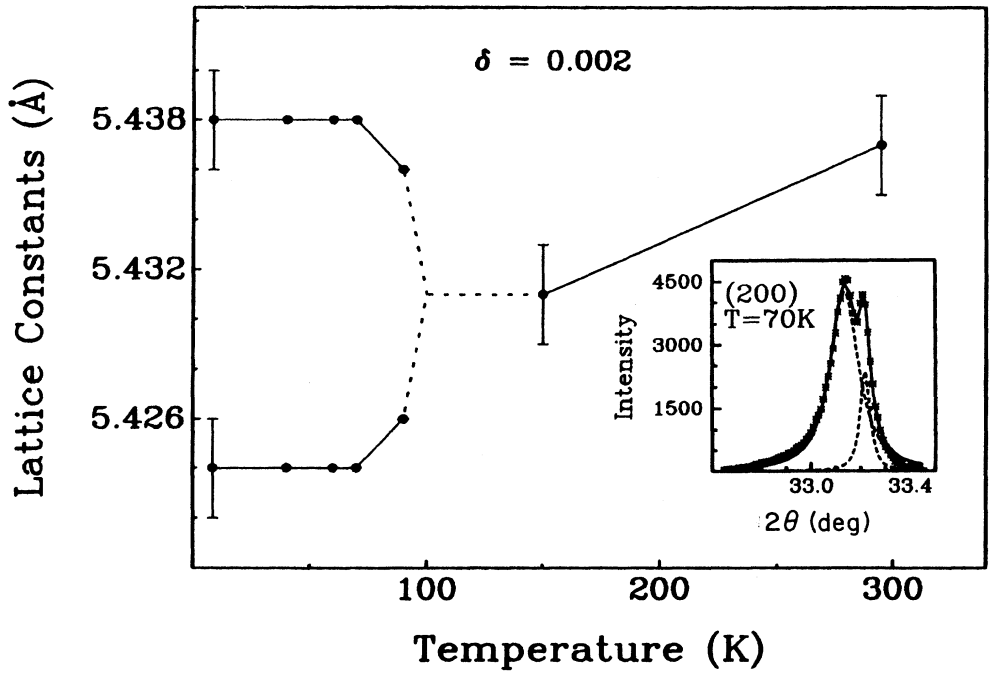

FIG 2. The a,b lattice constants measured by x-ray diffraction from $La_{1.80}Sr_{0.20}NiO_{4.002}$. The dashed lines are extrapolations from the data points to guide the eye. Inset: θ-2θ scan of the (200) reflection (orthorhombic B) at 70 K, showing the two-peak fit to the data.

saic misfit strain can change rapidly during thermal cycling. This may account for the irreproducible nature of the resistance anomalies described below.

IV. RESISTANCE

Resistance versus temperature measurements were made on oriented single-crystal specimens with excess oxygen values of $0.001 \leq \delta \leq 0.003$. The faces of the $4 \times 2 \times 1$-mm^3 specimens were oriented with the large face parallel to a (110) plane, and the sides along (001) and ($\bar{1}10$) planes. (Orthorhombic-*B* settings are used throughout.) Contacts were made to the four corners of the large face either by using silver paint to attach copper wires to evaporated silver pads, or by ultrasonically soldering copper wires directly with a Pb-Sn alloy solder. Using a computer-controlled scanner to interchange the current and voltage leads, resistances in both the [001] and the [$\bar{1}10$] directions were measured using the Montgomery method.[23] Specimen temperature was variable from room temperature to 5 K using a continuous-flow liquid-helium cryostat. Resistances typically exceeded 10^7 Ω as the temperature approached 20 K. Measurements at higher resistances were not reliable because of the input impedance of the voltmeter, although any low-resistance behavior at lower temperatures due to superconductivity would still have been observable (but was not seen). We eventually acquired a high input-impedance electrometer capable of measuring resistances in excess of 10^{12} Ω, which was used to measure resistance down to 5 K for one specimen with $\delta = 0.001$.

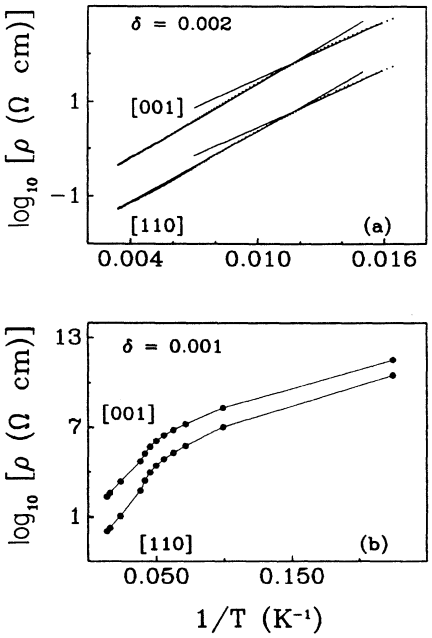

FIG. 4. Resistivity vs inverse temperature for $La_{1.80}Sr_{0.20}NiO_{4+\delta}$ showing activated behavior. Upper figure: $\delta = 0.002$, the high-temperature region from room temperature to 60 K, showing a small change in slope for the [110] and [001] current directions near 100 K, 50–41 meV, and 53–41 meV, respectively, from above to below 100 K. (Straight lines are shown to indicate changing slopes.) Lower figure: $\delta = 0.001$, the low-temperature region from 80 to 5 K, with [001] and [110] activation energies falling to 5 meV below 20 K.

All $La_{1.80}Sr_{0.20}NiO_{4+\delta}$ specimens had activated conductivity, with sample resistances exceeding 10^8 Ω below 10 K. The details of the *R* versus *T* curves and the deduced activation energies often changed as a sample was thermally cycled, but overall trends were readily discerned. Figure 4 shows representative results for both crystallographic directions. Note that there are several distinct changes with temperature.

Although data have been obtained from several specimens, we describe here a series of measurements made on the same sample. Resistance versus temperature was recorded simultaneously for both the [001] and the [$\bar{1}10$] current directions after oxygen annealing for δ values of 0.001, 0.002, and 0.003. By using the same sample, various sources of systematic error are eliminated. Several trends are clear from these measurements, which are summarized in Table I. These activation energies are obtained only from uninterrupted scans warming from below 20 K to room temperature. For both crystal directions, the activation energies are larger in the HTT phase than they are in the LTO phase. The activation energies also generally increase with increasing δ, although there is some scatter in the results.

Referring to the data for $\delta = 0.002$ shown in Fig. 4, above 100 K the *c*-axis activation energy is 53 meV, while the in-plane result is 50 meV. The anisotropy in the resistivity grows slightly throughout the temperature range, always having a value close to one decade. For comparison, the anisotropy in undoped La_2NiO_4 is greater than 10^2,[18] indicating that the presence of Sr reduces the two-dimensional character of this nickelate. Below the tetragonal-orthorhombic transition, the activation energy decreases to 41 meV for both directions. As shown in the $\delta = 0.001$ data (Fig. 4), both orientations have drastically reduced activation energies below 20 K, falling to 5 meV. This region of very small activation energies coincides with the rapid decrease of paramagnetic susceptibility and the onset of magnetic remanence (discussed below), indicating a transition to a new phase of electronic behavior. No evidence of a structural phase change was observed in the x-ray measurements.

The resistance data below 100 K often show discontinuous changes in the activation energies. A careful review of all of our results, however, revealed that most of these changes occurred when there was a pause in the

TABLE I $La_{1.80}Sr_{0.20}NiO_{4+\delta}$ activation energies in meV. These values were taken from the final warming cycle on the sample during which there were no stops and the rate of change in temperature was nearly constant. RT indicates room temperature.

	[110]		[001]	
δ	RT–100 K	< 100 K	RT–100 K	< 100 K
0.001	32	38	36	36
0.002	50	41	53	41
0.003	44	41	54	36

data collection, either to adjust the measuring current or for incidental reasons. (The measured resistances were found to be slightly current dependent, increasing by factors of 2 or 3 when the current was decreased from 10^{-3} to 10^{-5} A, for example.) These delays apparently induced changes in the specimens so that, in general, these results may not describe a material in thermodynamic equilibrium. One important exception is at the transition from tetragonal to orthorhombic structure near 100 K, where the distinct changes in activation energies were observed even when the data collection was uninterrupted, both in warming and cooling.

Several other specimens prepared under identical conditions underwent dramatic changes in resistance over narrow temperature ranges as shown in Fig. 5. In some cases the resistance fell by a factor of 1000 and then recovered to near the original value, all within a temperature range of a few degrees. Some specimens exhibited a more shallow drop in the resistance over a span of about 15 K. These effects could be observed repeatedly if the temperature was not changed too much, but they disappeared upon further thermal cycling. These irreproducible phenomena were always observed in the low-temperature orthorhombic phase, which was also shown by the x-ray rocking curve measurements to have an evolving mosaic structure dependent on time and temperature.

V. MAGNETIZATION

These investigations were motivated by the discovery of diamagnetism in the lanthanum nickelates by Kakol, Spałek, and Honig.[5,6] We have repeated their measurements on identically prepared specimens using the same vibrating sample magnetometer (VSM) and have observed similar magnetic behavior. In some cases the specimen resistance was measured along with the magnetization, which revealed that the diamagnetism coexists with a semiconducting-insulating state of conductivity.

Figure 6 shows the results for a 130-mg $La_{1.80}Sr_{0.20}NiO_{4.002}$ specimen with a 12-kOe field parallel to the [001] direction. Electrical contacts were attached to the specimen in a four-probe configuration for resistance measurements, which were made in zero field after each measurement of the magnetization. As the sample was first cooled from room temperature down to 4.2 K, a characteristic paramagnetic peak was observed near 20 K. The data in Fig. 6 were then taken upon slowly warming from 4.2 to 64 K, where a small decrease in magnetization was observed, and then cooling back to 4.2 K. For each temperature value, the applied field was increased, magnetization was measured, and the field was reduced back to zero again. This procedure is typical for those specimens which exhibit diamagnetism; the annealing temperature of 64 K may be related to the value at which the orthorhombic a/b ratio reaches its maximum value (Fig. 2). While all specimens have a paramagnetic peak at 20 K and a decreasing susceptibility with diminishing temperature, most specimens are not yet diamagnetic at 4.2 K. We did not discover a systematic method for achieving diamagnetism, relying instead on trial and error.

If one assumes that the maximum diamagnetic moment of 7.4×10^{-3} emu is due to conventional superconductivity, the deduced magnetic susceptibility χ corresponds to 0.041% of $(1/4\pi)$, the susceptibility of an ideal superconductor. Therefore, only a very small fraction of the specimen could be superconducting if conventional superconductivity is responsible for the diamagnetism. The

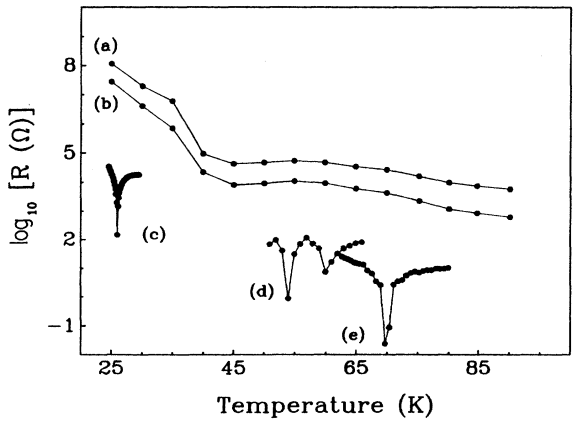

FIG. 5. Examples of resistance anomalies observed in several specimens of $La_{1.80}Sr_{0.20}NiO_{4+\delta}$. (a) and (b) are the [001] and [110] resistances measured simultaneously from one specimen, while (c)–(e) show results from other specimens, each with the current flowing in the [110] direction.

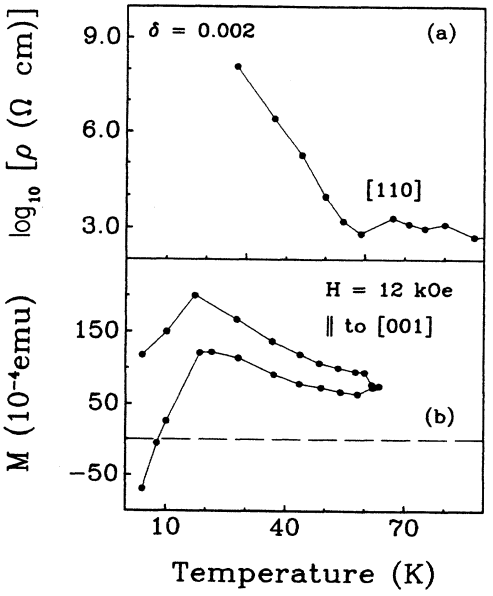

FIG. 6. Resistivity (above) and magnetization (below) vs temperature for a single crystal of $La_{1.80}Sr_{0.20}NiO_{4.002}$. Resistance was measured with zero applied magnetic field, in between measurements of the magnetization. Note the negative moment for an applied field in the [001] direction below 10 K. The resistivity exceeds 10^7 Ω cm below 30 K.

resistance increased with typical semiconducting behavior until it exceeded 10^8 Ω near 20 K, the upper limit of the apparatus. The resistance remained above 10^8 Ω for all temperatures below 20 K, including the diamagnetic region. While this obviously shows that the sample as a whole is not superconducting, we cannot rule out the presence of a minute superconducting fraction below the percolation threshold.

VI. DISCUSSION

The lattice constant and magnetization measurements provide a straightforward description of $La_{1.80}Sr_{0.20}NiO_{4+\delta}$. From room temperature down to 100 K this material has a tetragonal structure and is paramagnetic. Between 100 and 20 K the paramagnetic moment gradually increases, and the structure is orthorhombic with an a/b ratio of 1.0026. Below 20 K the susceptibility steadily decreases, becoming diamagnetic above 4.2 K in some cases. At the same time the remanent magnetic moment becomes finite, consistent with a high-temperature antiferromagnetic ordering becoming slightly ferrimagnetic. No change in lattice constants was detected.

These simple observations are in stark contrast to the rather complicated electrical resistance found in these three temperature regions. At high temperatures the c-axis resistivity always shows activated conductivity with a constant activation energy of 35–54 meV. The in-plane behavior was similar, showing a constant activation energy of 32–50 MeV. The middle temperature region is the least predictable, with activation energies abruptly changing during pauses in the measurements, and occasional sudden drops of several orders of magnitude which recover in a few degrees. In general, the activation energies are smaller in the intermediate phase than they are at higher temperatures, but exceptions were found, as shown by the $\delta=0.001$ data in Table I. This temperature region also shows drastic changes in x-ray rocking curves, apparently due to strain between orthorhombic mosaic domains. The resistivity in the lowest temperature region is very high, in excess of 10^{10} Ω cm. In one measurement permitting accurate determinations up to 10^{11} Ω at 4.2 K, the activation energies had fallen drastically to 5 meV, with no sign of the anomalies common to the middle region.

A schematic band-structure model to explain the conductivity in La_2NiO_4 was proposed by Goodenough and Ramasesha,[24] and was extended by Buttrey *et al.*[25] The bands near the Fermi level are assumed to be due to Ni d electrons. The orbitals in the c-axis direction are highly localized, forming narrow bands, while the in-plane orbitals have a substantial overlap. In the absence of magnetic correlations, the Fermi level would intersect these in-plane d bands to form a metal. Since the undoped lanthanum nickelate has an activated conductivity and is antiferromagnetic as well, the presence of magnetic ordering was assumed to create a gap at the Fermi level comparable in size with the Néel temperature. These concepts can be easily extended to the Sr-doped materials in this study. The variability of the activation energies clearly shows that the gap about the Fermi level is very sensitive to the magnetic ordering and perhaps such factors as mosaic strain as well. The magnetic ordering itself was quite repeatable, with every specimen showing similar paramagnetic susceptibilities, gradually building up to a peak at 20 K and followed by a steady decline at lower temperatures, although the presence of diamagnetic susceptibility above 4.2 K was unpredictable. The presence of diamagnetic susceptibility in both the doped and undoped nickelates[5,6] is not accounted for in this simple model.

VII. CONCLUSIONS

This work was undertaken to explore the structure and transport properties of $La_{1.80}Sr_{0.20}NiO_{4+\delta}$ in light of the discovery of diamagnetism[5,6] and the similarity with superconducting lanthanum cuprates. These efforts were confined to well-characterized single-crystal specimens with oxygen contents close to stoichiometry, i.e., $0.001 \leq \delta \leq 0.003$. We find that the weak diamagnetic susceptibility coexists with electrical resistivity in excess of 10^{10} Ω cm, with no other evidence for a superconducting fraction of the specimen. The high-temperature tetragonal phase was found to transform to the low-temperature orthorhombic structure near 100 K. The variability of the activation energies indicates that the electronic band gap at the Fermi level is very sensitive to magnetic ordering and perhaps mosaic strain. These materials are difficult subjects for study because of this unstable nature, but they are unusually rich in structural, resistive, and magnetic behavior. The physical origin of the observed diamagnetism in these high-resistance materials, in particular, invites further investigation.

ACKNOWLEDGMENTS

We gratefully acknowledge the role of J. Honig in nearly all aspects of understanding the lanthanum nickelates. We also thank Z. Kakol for guidance with the VSM measurements, and J. Spałek for helpful discussions. P. Metcalf was most helpful with several aspects of sample preparation, especially the precision oxygen annealing. The crystals were grown by M. Wittenauer, D. Buttrey, and R. Shartman. Funding was provided by the Indiana Center for Innovative Superconducting Technology, the National Science Foundation through Grant No. DMR 8657587, and by the Department of Energy through Grant No. DE-FG02-85-ER45183. Research carried out in part at the National Synchrotron Light Source, Brookhaven National Laboratory, which is supported by the U.S. Department of Energy, Division of Materials Sciences and Division of Chemical Sciences. S.A.H. acknowledges the support of the Kodak Foundation.

[1]J. G. Bednorz and K. A. Muller, Z. Phys. B **64**, 189 (1986).
[2]G. Aeppli, D. R. Harshman, D. Buttrey, E. Ansaldo, G. P. Espinosa, A. S. Cooper, J. P. Remeika, T. Freltoft, T. M. Riseman, D. R. Noakes, B. Ellman, T. F. Rosenbaum, and D. L. Williams, Physica C **153-155**, 1111 (1988).
[3]G. Aeppli and D. J. Buttrey, Phys. Rev. Lett. **61**, 203 (1988).
[4]J. Rodríquez-Carvajal, J. L. Martínez, J. Pannetier, and R. Saez-Puche, Phys. Rev. B **38**, 3148 (1988).
[5]Z. Kakol, J. Spałek, and J. M. Honig, J. Solid State Chem. **79**, 288 (1989).
[6]Z. Kakol, J. Spałek, and J. M. Honig, Solid State Commun. **71**, 283 (1989).
[7]H. R. Harrison, R. Aragon, and C. J. Sandberg, Mater. Res. Bull. **15**, 571 (1980).
[8]R. Schardtman, Ph. D. thesis, Purdue University, 1988 (unpublished).
[9]J. Fontcuberta, G. Langworth, and J. B. Goodenough, Phys. Rev. B **30**, 6320 (1984).
[10]G. H. Lander, P. J. Brown, J. Spałek, and J. M. Honig, Phys. Rev. B **40**, 4463 (1989).
[11]J. D. Jorgensen, B. Dabrowski, S. Pei, D. R. Richards, and D. G. Hinks, Phys. Rev. B **40**, 2187 (1989).
[12]J. D. Jorgensen, B. Dabrowski, S. Pei, D. G. Hinks, L. Soderholm, B. Morosin, J. E. Schirber, E. L. Venturini, and D. S. Ginley, Phys. Rev. B **38**, 11 337 (1988).
[13]J. D. Jorgensen, H. -B. Schüttler, D. G. Hinks, D. W. Capone, II, K. Zhang, M. B. Brodsky, and D. J. Scalapino, Phys. Rev. Lett. **58**, 1024 (1987).
[14]D. McK. Paul, G. Balakrishnan, N. R. Bernhoeft, W. I. F. David, and W. T. A. Harrison, Phys. Rev. Lett. **58**, 1976 (1987).
[15]J. D. Axe, A. H. Moudden, D. Hohlwein, D. E. Cox, K. M. Mohanty, A. R. Moodenbaugh, and Y. Xu, Phys. Rev. Lett. **62**, 2751 (1989).
[16]*International Tables for X-Ray Crystallography,* edited by Norman F. M. Henry and Kathleen Lonsdale (Kynoch, Birmingham, England, 1969), Vol. 1.
[17]Gerald Burns and A. M. Glazer, *Space Groups for Solid State Scientists* (Academic, New York, 1978).
[18]C. N. R. Rao, D. J. Buttrey, N. Otsuka, P. Ganguly, H. R. Harrison, C. J. Sandberg, and J. M. Honig, J. Solid State Chem. **51**, 266 (1984).
[19]G. Aeppli and D. J. Buttrey, Phys. Rev. Lett. **61**, 203 (1988).
[20]J. M. Longo and P. M. Raccah, J. Solid State Chem. **6**, 529 (1973).
[21]Von B. Grande, H. K. Muller-Buschbaum, and M. Schweizer, Z. Anorg. Allg. Chem. **428**, 120 (1977).
[22]M. M. Hall, V. G. Veeraraghavan, H. Rubin, and P. G. Winchell, J. Appl. Cryst. **10**, 66 (1977).
[23]H. C. Montgomery, J. Appl. Phys. **42**, 2971 (1971).
[24]J. B. Goodenough and S. Ramasesha, Matter Res. Bull. **17**, 383 (1982).
[25]D. J. Buttrey, J. M. Honig, and C. N. R. Rao, J. Solid State Chem. **64**, 287 (1986).